

SrAlOCl:Bi³⁺@SiO₂ phosphor with broad emission band and its effects on LED optical power and correlated color temperature

Ha Thanh Tung¹, Huu Phuc Dang², Hoang Thinh Nhan³

¹Faculty of Basic Sciences, Vinh Long University of Technology Education, Vinh Long Province, Vietnam

²Faculty of Fundamental Science, Industrial University of Ho Chi Minh City, Ho Chi Minh City, Vietnam

³Faculty of Engineering and Technology, Nguyen Tat Thanh University, Ho Chi Minh City, Vietnam

Article Info

Article history:

Received Oct 6, 2022

Revised Nov 2, 2022

Accepted Nov 27, 2022

Keywords:

Color deviation

Color quality scale

Color rendering index

Luminescence intensity

Sr₃Al₂O₅Cl₂:Bi³⁺

ABSTRACT

Sr₃Al₂O₅Cl₂:Bi³⁺ (SAIOCl:Bi³⁺) phosphor for broadband emission was made using a solid-state method. From the extensive spectroscopic analysis and theoretical computation, significant conclusions about the origin of the Bi³⁺ emission were drawn. For the Sr 3 and Sr 1 sites, respectively, the dipole-quadrupole and quadrupole-quadrupole interactions were responsible for the concentration quenching in SAIOCl:Bi³⁺. The resulting luminescence mechanism demonstrated that the crystallization of Bi³⁺ at the two sites is what causes the emission from each site. The warm white light emitting diodes (LED) models were built with a 380 nm ultraviolet (UV) chip, SAIOCl:Bi³⁺, and two other phosphors. Then, the color rendering indices (CRI) and the correlated color temperature (CCT) were calculated. Particularly, the CRI values ranged from 84.3 to 86.2 under operating currents of 20–50 mA, respectively. The increasing SAIOCl:Bi³⁺ dosage also heightened particle density, resulting in higher scattering coefficients. High scattering results in improved color coordination (lower color variance). The CRI and luminous flux are reduced as the phosphor SAIOCl:Bi³⁺ concentration increases more than owing to color loss and energy loss by backscattering and re-absorption. Thus, it is advisable to consider SAIOCl:Bi³⁺ carefully before applying in production.

This is an open access article under the [CC BY-SA](https://creativecommons.org/licenses/by-sa/4.0/) license.



Corresponding Author:

Huu Phuc Dang

Faculty of Fundamental Science, Industrial University of Ho Chi Minh City

No. 12 Nguyen Van Bao Street, Ho Chi Minh, Vietnam

Email: danghuuphuc@iuh.edu.vn

1. INTRODUCTION

White light emitting diodes (LEDs) have been emerged and commercially applied in solid-state lighting applications, such as in traffic lights, light streets, interior lighting in transportation vehicles like airplane, cars or buses, and in liquid-crystal display (LCD) [1]. The LED widely applied for this solid-state technology were obtained by using III-nitride-based LED chip combined with YAG:Ce³⁺ phosphor to provide essential blue and yellow emissions for white-light generation. Then, the white LED (WLED) with higher luminescence performance was presented, which was acquired using the combination of red, blue, or green phosphors, and an ultraviolet (UV) chip. Besides, the phosphor material offering broad emission band have been the focus of recent research on luminescent and color improvements [2], [3]. Bi³⁺ doped phosphors have various potential optoelectronic features because of the strong interactions of Bi³⁺ with the host lattice [4], [5]. Bi³⁺ can be excited easily in near-UV region rather than visible-light region, effectively minimized the reabsorption of light. The rare-earth doped phosphors, on the other hand, usually emits light in the blue-green wavelengths, leading to large reabsorption, causing the significant degradation in LED luminosity.

Thus, Bi^{3+} is more advantageous than rare-earth ions when using as a dopant to stimulate the phosphor luminescence efficiency. Additionally, Bi^{3+} ions can provide the emission spectra ranging from near-UV to red, depending on the host lattice. Besides, Bi^{3+} luminescence depends much on the surrounding crystal field and coordination environment [6]. Thus, the choice of phosphor host is important. $\text{Sr}_3\text{Al}_2\text{O}_5\text{Cl}_2$ (SrAlOCl) has three types of cation lattice locations that can affect the fluorescence, and also a phosphor host with high chemical and thermal stabilities. Thus, SrAlOCl is a good host for many ions, including Eu^{2+} , Ce^{3+} , Li^+ , Tm^{3+} , Tb^{3+} , and Pr^{3+} [7], [8]. However, there are little research focus on the dopant Bi^{3+} in SrAlOCl host [9].

In this study, a Bi^{3+} -doped SrAlOCl phosphor is introduced and investigated. The phosphor was prepared with a solid-state synthesizing method. The phosphor primary emission shifted from 490-556 nm as the Bi^{3+} concentration increased, indicating the dependence on dopant concentration of the phosphor emissions. Assuming that two of the three types of crystal field environments—Sr 1 and Sr 3 sites—participated in the fluorescence process and had coordination numbers of 8 and 7, respectively, the luminescence properties in these Sr sites are demonstrated. Besides, the $\text{SrAlOCl}:\text{Bi}^{3+}$ phosphor with yellow-green emission is combined with a UV LED chip (380 nm) and other two phosphor types. The color rendition values were collected from 84.3 to 86.2 with increasing working currents from 20-50 mA, respectively. Thus, the phosphor $\text{SrAlOCl}:\text{Bi}^{3+}$ is a good candidate for generating warm-WLED lamps.

2. METHOD

2.1. Materials preparation

The $\text{SrAlOCl}:\text{Bi}^{3+}$ phosphor was prepared with the solid-state synthesizing technique at high temperature. The raw ingredients and essential agents for the synthesis were listed in Table 1. All listed substances were precisely weighed in stoichiometry. Next, they went through a 4 minute grinding process in an agate mortar. Subsequently, the ground compound was put in an agate mortar and went through 4 hour sintering at 1,200 °C. Then, it was removed out of the mortar once the temperature fell to room temperature (roughly 25 °C). Subsequently, the mixture was ground again and placed in a reagent bottle to be used in the subsequent measurement [10].

Table 1. Ingredients of $\text{SrAlOCl}:\text{Bi}^{3+}$ phosphor

Raw	Agents
SrCO_3	Li_2CO_3 (CC)
Al_2O_3	Na_2CO_3 (CC)
$\text{SrCl}_2 \cdot 6\text{H}_2\text{O}$	K_2CO_3 (CC)
Bi_2O_3	NH_4Cl (Fx)
	BaF_2 (Fx)
	H_3BO_3 (Fx)
CC: charge compensating	
Fx: fluxing	

2.2. Instruments

Using a Bruker D8 Phaser diffractometer at 40 kV voltage and $\text{Cu K}\alpha$ radiation of 1.0546 Å, we measured the X-ray diffraction patterns of the phosphor samples [11], [12]. In order to present the Rietveld refinement investigation, GSAS software and EXPGUI interface were applied. The spectral luminescence of the as-prepared phosphor was measured using a Hitachi F-7,000 fluorescence spectrophotometer having an excitation source as a 150 W xenon lamp. The spectral diffuse reflectance was determined using a Hitachi U-4,100 UV-vis spectro-photometer. The fluorescence lifetimes were measured using a Horiba Fluorolog-3. For the examination of the phosphor surface morphology, a Nova Nano SEM450 from Field Electron and Ion (FEI) company was employed. Every measurement was carried out at room temperature.

2.3. WLED simulation

The phosphor of $\text{SrAlSiN}_3:\text{Eu}^{2+}$ (620 nm), $\text{BaMgAl}_{10}\text{O}_{17}:\text{Eu}^{2+}$ (466 nm), and $\text{SrAlOCl}:\text{Bi}^{3+}$ (with 5% Bi^{3+}) phosphors were blended with epoxy glue to form a luminescent film in addition to the YAG:Ce phosphor one. The phosphor films were placed onto UV chips (380 nm). We measured the chromaticity coordinate, correlated color temperature (CCT), and color rendering R_a , color quality scale (CQS) using an integrating sphere. These parameters were discussed together with the luminescence of the WLED for demonstrating the effect of $\text{SrAlOCl}:\text{Bi}^{3+}$ and its concentration. The simulation illustration of the WLED is illustrated in Figure 1, with Figure 1(a) showing the real fabricated WLED model, Figure 1(b) and

Figure 1(c) showing the bonding diagram and 2D cross-section of the WLED model, respectively, and Figure 1(d) demonstrating the 3D-built model of the WLED by LightTools software [13], [14].

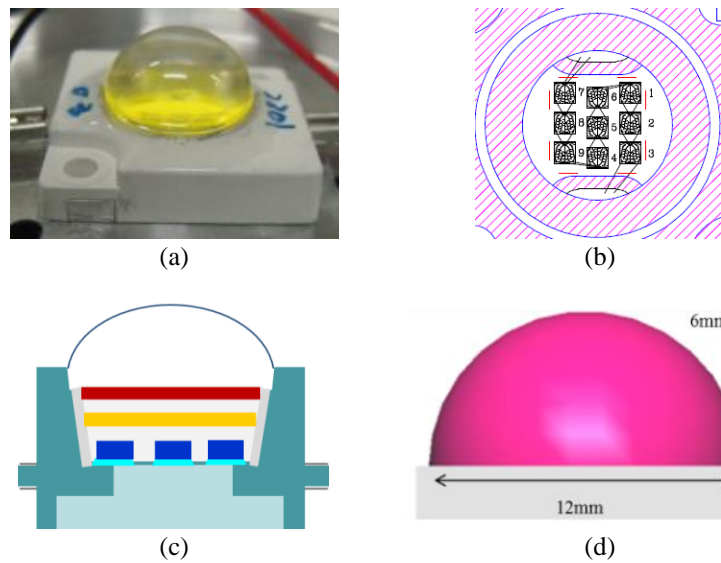


Figure 1. Photograph of WLEDs structure (a) actual WLEDs, (b) bonding diagram, (c) illustration of pc-WLEDs model, and (d) simulation of WLEDs using lighttools commercial software

2.4. Computation

The computation framework based on density-function theory was constructed using vienna ab-initio simulation package (VASP). SrAlOCl system energy and separate Sr sites were computed and transferred into relative numbers. The energy bandgap of SrAlOCl was also calculated using a Vanderbilt-type ultrasoft pseudopotential formalism and exchange-correlation function based on the Perdew-Burke-Ernzerhof (PBE) generalized gradient approximation. When doping ion Bi^{3+} into the host SrAlOCl, the substitution of Bi^{3+} with Sr^{2+} is likely to occurred. This substitution creates bivalent vacancy (V_{Sr}'') in the host, as shown in (1). As the Bi^{3+} ion has smaller particle size than that of the Sr^{2+} ion, after Bi^{3+} is added into SrAlOCl as an activated ion, the lattice parameters are smaller, according to the demonstration of bragg summarized in (2) [15], [16].



$$2d \sin \theta = n\lambda n = 1, 2, 3, \dots \quad (2)$$

where, Bi_{Sr} is the occupation space of Bi^{3+} in the host; d represents the interplanar spacing of the crystals, θ indicates the angle between X-ray incident and crystal face, and n and λ indicate the X-ray incident wavelength and order of diffraction, respectively.

The energy transfer between Bi^{3+} ions happen as we increase the ion doping concentration, which causes the broadband yellow-green emission of the phosphor to be stronger. The critical distance of identifying the energy transferring mechanism among the ions can be obtained using blasse equation, as (3). Here, the critical distance parameter is represented by R_c and has the unit cell volume (V), the number of cations in the unit cell (N), and the critical concentration (X_c) [17]–[19].

$$R_c \approx 2 \left(3V / 4\pi X_c N \right)^{1/3} \quad (3)$$

where, V and N are equal to 0.836 nm^3 and 4, respectively; the critical concentration X_c are 0.008 (490 nm) and 0.5 mol (556 nm). Thus, the calculated R_c are 1.999 (490 nm) and 3.681 (556 nm), all of which are greater than 0.5 nm. With this result, interaction that is responsible for the Bi^{3+} energy transfer is the multipolar one. Utilizing the energy-resonance expression by Dexter, it is possible to identify these interactions [20]–[23].

3. RESULTS AND DISCUSSION

Figure 2 shows the number density as a function of varying SrAlOCl:Bi^{3+} phosphor concentration. At the same particle size ($1\mu\text{m}$), the number density of phosphor particles increases with the increasing concentration (5%-25%) of the phosphor. Figures 2(a)-(e) displays phosphor concentration at 5%, 10%, 15%, 20%, and 25%, respectively. The increasing in number density of phosphor particles indicates the changes in light scattering within the WLED model. Figure 3 illustrates the changes in yellow-phosphor YAG:Ce concentration as the SrAlOCl:Bi^{3+} concentration increases. The reduction in YAG:Ce concentration is clearly observed, which play a critical role in maintain stable correlated color temperatures–CCTs of the WLED [24], [25]. In addition, the reduction of yellow phosphor YAG:Ce contributes to changes the scattering and absorption properties of emitted light from the chip and phosphors. Such changes probably affect the color rendition and luminous output of the WLED.

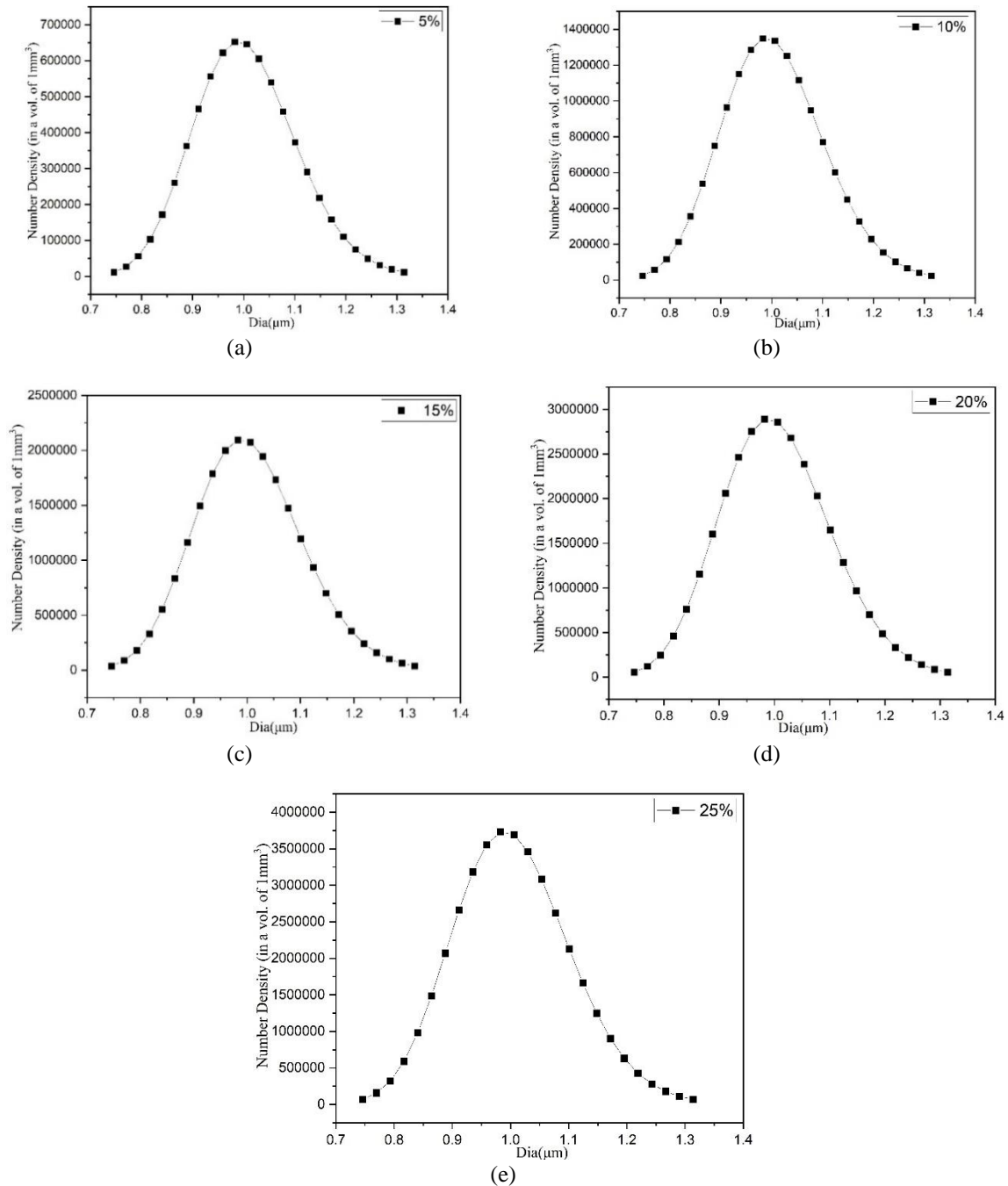


Figure 2. Number density of $\text{SrAlOCl:Bi}^{3+}@SiO_2$ as a function of varying phosphor concentration (a) 5%, (b) 10%, (c) 15%, (d) 20%, and (e) 25%

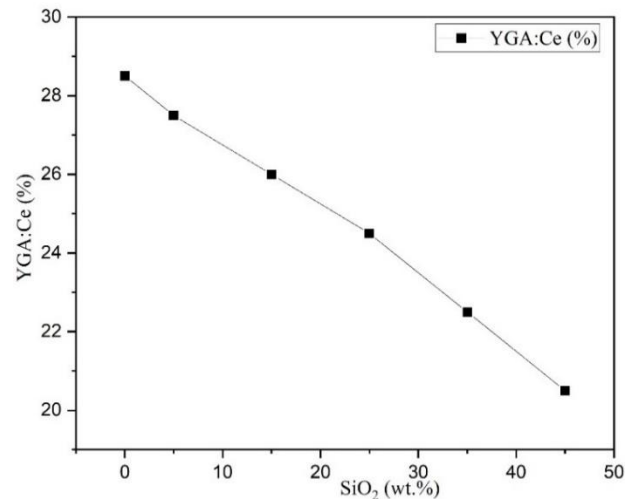


Figure 3. YGA:Ce decreases as a function of varying SrAlOCl:Bi³⁺@SiO₂ concentration

Figure 4 shows the CCT changes in connection with the varying concentration of SrAlOCl:Bi³⁺. The results show that growing the concentration of SrAlOCl:Bi³⁺ phosphor leads to the relatively decreases in CCT values as the scattering efficiency of the phosphor increases. The increase in scattering leads the enhancement in emission intensity of the phosphor. Especially, when 25% SrAlOCl:Bi³⁺ is used, the CCT is relatively stable, the deviation between the max and min values shows to be the smallest, which can be seen obviously in Figure 5. As a result, it is possible to use up to 25% SrAlOCl:Bi³⁺ to obtain the highest color coordination. The CCT values of the WLED are acquired using the (4) [26],

$$CCT = 437n^3 + 3601n^2 + 6831n + 5517 \quad (4)$$

where n represents the intermediate variable equal to $(x - 0.3320)/(0.1858 - y)$ with y and x collected from the CIE coordinate. With varying currents, the CCT is different; specifically, 4326 K for 20 mA, 4319 K for 30 mA, 4297 K for 40 mA, and 4270 K for 50 mA. From these results, the generated white light we recorded is warm white light. Besides, with the increasing currents (20–50 mA), the color rendering values R_a also increases from 84.3 to 86.2, respectively, indicating the improvement in color rendition of WLED when using Bi³⁺-activated SrAlOCl yellow-green phosphor.

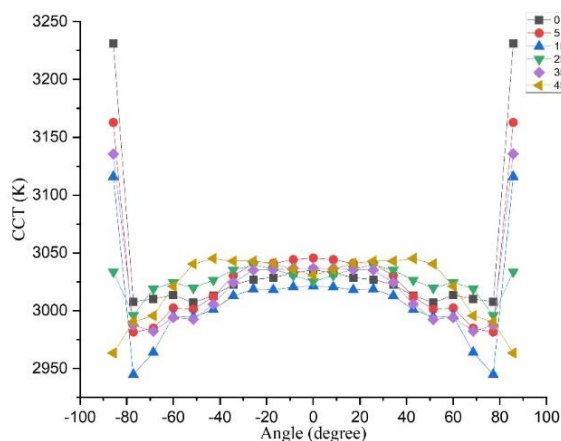


Figure 4. CCT changes as a function of varying SrAlOCl:Bi³⁺@SiO₂ concentration

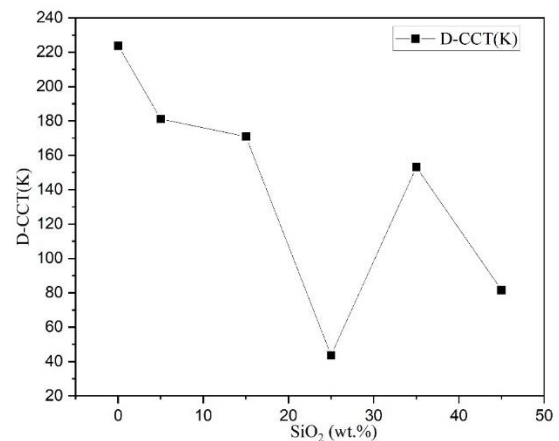


Figure 5. Color variance as a function of varying SrAlOCl:Bi³⁺@SiO₂ concentration

Figures 6 and 7 show the luminous intensity and emission spectra of the WLED with the variation in SrAlOCl:Bi³⁺ concentration, respectively. As in Figure 6, the slight increase of the phosphor concentration,

from 0 to 5%, causes a slight increase in luminosity. This could be attributed to the enhancement in phosphor emission intensity as the scattering is properly improved. Then the luminous flux suddenly drops as the concentration increases owing to the redundant scattering. When more emission light scatterings happen, the luminous flux is reduced because the chip-emitted light is scattered back to the LED chip surface and re-absorbed. Figure 7 showed that the addition of the SrAlOCl:Bi^{3+} phosphor contributes to promote the emission light of the package, especially within the yellow-green region.

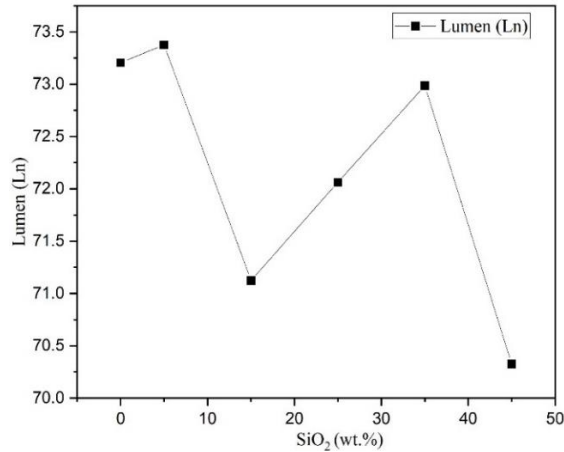


Figure 6. Lumen output as a function of varying $\text{SrAlOCl:Bi}^{3+}@\text{SiO}_2$ concentration

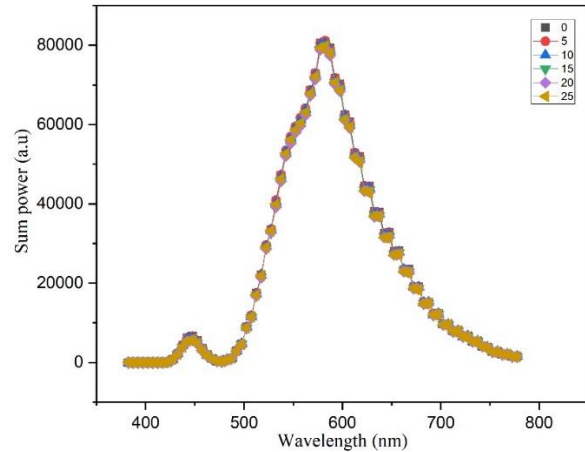


Figure 7. Luminescent spectra of WLED as a function of varying $\text{SrAlOCl:Bi}^{3+}@\text{SiO}_2$ concentration

Figures 8 and 9 show the color rendering indices (CRI) and CQS values of the WLED regarding the changes in SrAlOCl:Bi^{3+} concentration. Two figures exhibit that increasing concentration of SrAlOCl:Bi^{3+} will harm the CRI and CQS as the light is shifted to yellow-green region, owing to the increase in phosphor emission light by improved scattering. The increase in concentration induces the scattering events, especially that of the blue light, according to Mie scattering. Thus, the blue light when reaching the phosphor layers is converted into the yellow-greenish light, which continues to scatter and combine with other yellow light from the YAG:Ce phosphor. This means the blue emission from the chip would be shortage to form white light, resulting in the light generated in other color, such as green light. Therefore, the redundant scattering will degrade the CRI and CQS.

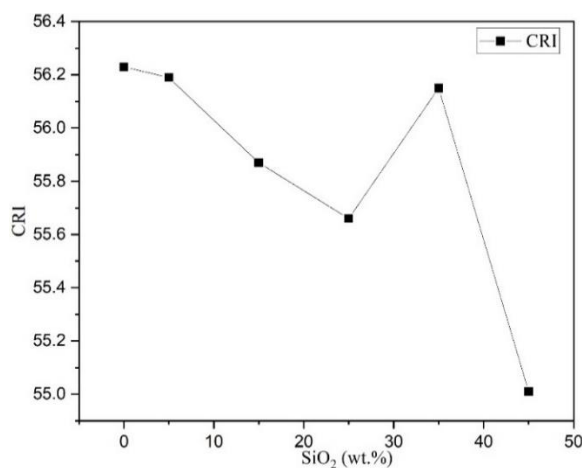


Figure 8. CRI performance as a function of varying $\text{SrAlOCl:Bi}^{3+}@\text{SiO}_2$ concentration

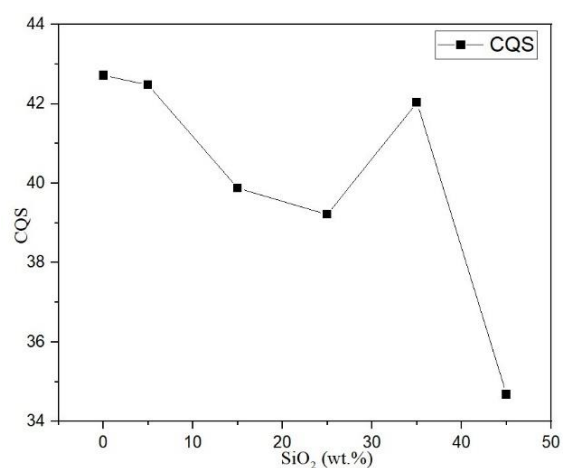


Figure 9. CQS values as a function of varying $\text{SrAlOCl:Bi}^{3+}@\text{SiO}_2$ concentration

4. CONCLUSION

In conclusion, the solid-state approach was used to prepare the broadband emission SrAlOCl:Bi^{3+} phosphor. Important findings regarding the source of the Bi^{3+} emission were gained from the thorough spectroscopic investigation and theoretical computation. The dipole-quadrupole and quadrupole-quadrupole interactions for the Sr 3 and Sr 1 sites, respectively, caused the concentration quenching in SrAlOCl:Bi^{3+} . As a result, the luminescence mechanism was presented, showing that the emission from the two sites results from the crystallization of Bi^{3+} at two different lattice sites. By CCT calculating, the color rendition values Ra of the warm WLED built with a 380 nm UV chip, SrAlOCl:Bi^{3+} , and other two phosphors, were obtained. Specifically, the CRI values were obtained from 84.3 to 86.2 under 20–50 mA operating currents, respectively. Furthermore, when growing the phosphor concentration of SrAlOCl:Bi^{3+} , the number density of the particles increases, leading to the higher scattering coefficients. High scattering leads to better color coordination (lower color variance). The color rendition is reduced if the scattering is too much since the blue light is scattered most and more green lights to be converted. The luminosity degraded with increasing SrAlOCl:Bi^{3+} concentration, owing to the increases in backscattering and the number density increases and the blue-light energy loss during to re-absorption. Thus, the SrAlOCl:Bi^{3+} concentration should be consider carefully before applying in production.




REFERENCES

- [1] S. Sadeghi, B. G. Kumar, R. Melikov, M. M. Aria, H. B. Jalali, and S. Nizamoglu, "Quantum dot white LEDs with high luminous efficiency," *Optica*, vol. 5, no. 7, pp. 793–802, Jul. 2018, doi: 10.1364/OPTICA.5.000793.
- [2] F.-B. Chen, K.-L. Chi, W.-Y. Yen, J.-K. Sheu, M.-L. Lee, and J.-W. Shi, "Investigation on modulation speed of photon-recycling white light-emitting diodes with vertical-conduction structure," *Journal of Lightwave Technology*, vol. 37, no. 4, pp. 1225–1230, Feb. 2019, doi: 10.1109/JLT.2018.2890331.
- [3] N. D. Q. Anh, P. X. Le, and H. Y. Lee, "Selection of a remote phosphor configuration to enhance the color quality of white LEDs," *Current Optics and Photonics*, vol. 3, no. 1, pp. 78–85, 2019, doi: 10.3807/COPP.2019.3.1.078.
- [4] L. Wang, X. Wang, J. Kang, and C. P. Yue, "A 75-Mb/s RGB PAM-4 visible light communication transceiver system with pre- and post-equalization," *Journal of Lightwave Technology*, vol. 39, no. 5, pp. 1381–1390, 2021, doi: 10.1109/JLT.2020.3034227.
- [5] R. Wan *et al.*, "Nanohole array structured GaN-based white LEDs with improved modulation bandwidth via plasmon resonance and non-radiative energy transfer," *Photonics Research*, vol. 9, no. 7, pp. 1213–1217, 2021, doi: 10.1364/PRJ.421366.
- [6] M. Talone and G. Zibordi, "Spatial uniformity of the spectral radiance by white LED-based flat-fields," *OSA Continuum*, vol. 3, no. 9, pp. 2501–2511, 2020, doi: 10.1364/OSAC.394805.
- [7] Y. Ma *et al.*, "Broadband emission Gd³⁺ Sc³⁺ Al³⁺ O₁₂:Ce³⁺ transparent ceramics with a high color rendering index for high-power white LEDs/LDs," *Optics Express*, vol. 29, no. 6, pp. 9474–9493, 2021, doi: 10.1364/OE.417464.
- [8] Y. Li, X. Zhang, H. Yang, X. Yi, J. Wang, and J. Li, "Effects of remote sediment phosphor plates on high power laser-based white light sources," *Optics Express*, vol. 29, no. 15, pp. 24552–24560, 2021, doi: 10.1364/OE.433581.
- [9] Q. Guo *et al.*, "Characterization of YAG:Ce phosphor dosimeter by the co-precipitation method for radiotherapy," *Applied Optics*, vol. 60, no. 11, pp. 3044–3048, 2021, doi: 10.1364/AO.419800.
- [10] E. Chatzizyrlis, M. Hinkelmann, A. Afentaki, R. Lachmayer, J. Neumann, and D. Kracht, "Optimizing the laser diode ray tracing model for LERP system simulation based on likelihood image sampling," in *2021 Conference on Lasers and Electro-Optics Europe & European Quantum Electronics Conference (CLEO/Europe-EQEC)*, 2021, doi: 10.1109/CLEO/Europe-EQEC52157.2021.9542784.
- [11] H. Daicho, K. Enomoto, H. Sawa, S. Matsuishi, and H. Hosono, "Improved color uniformity in white light-emitting diodes using newly developed phosphors," *Optics Express*, vol. 26, no. 19, pp. 24784–24791, 2018, doi: 10.1364/OE.26.024784.
- [12] I. G. Palchikova, E. S. Smirnov, and E. I. Palchikov, "Quantization noise as a determinant for color thresholds in machine vision," *Journal of the Optical Society of America A*, vol. 35, no. 4, pp. 214–222, 2018, doi: 10.1364/JOSAA.35.00B214.
- [13] W. J. Kim *et al.*, "Improved angular color uniformity and hydrothermal reliability of phosphor-converted white light-emitting diodes by using phosphor sedimentation," *Optics Express*, vol. 26, no. 22, pp. 28634–28640, 2018, doi: 10.1364/OE.26.028634.
- [14] Z. Zhao, H. Zhang, S. Liu, and X. Wang, "Effective freeform TIR lens designed for LEDs with high angular color uniformity," *Applied Optics*, vol. 57, no. 15, pp. 4216–4221, 2018, doi: 10.1364/AO.57.004216.
- [15] T. Hu *et al.*, "Demonstration of color display metasurfaces via immersion lithography on a 12-inch silicon wafer," *Optics Express*, vol. 26, no. 15, pp. 19548–19554, 2018, doi: 10.1364/OE.26.019548.
- [16] S.-W. Jeon *et al.*, "Optical design of dental light using a remote phosphor light-emitting diode package for improving illumination uniformity," *Applied Optics*, vol. 57, no. 21, pp. 5998–6003, 2018, doi: 10.1364/AO.57.005998.
- [17] Z. Li, Y. Tang, J. Li, X. Ding, C. Yan, and B. Yu, "Effect of flip-chip height on the optical performance of conformal white-light-emitting diodes," *Optics Letters*, vol. 43, no. 5, pp. 1015–1018, 2018, doi: 10.1364/OL.43.001015.
- [18] E. Chen *et al.*, "Flexible/curved backlight module with quantum-dots microstructure array for liquid crystal displays," *Optics Express*, vol. 26, no. 3, pp. 3466–3482, 2018, doi: 10.1364/OE.26.003466.
- [19] Y.-F. Huang, Y.-C. Chi, M.-K. Chen, D.-P. Tsai, D.-W. Huang, and G.-R. Lin, "Red/green/blue LD mixed white-light communication at 6500K with divergent diffuser optimization," *Optics Express*, vol. 26, no. 18, pp. 23397–23410, 2018, doi: 10.1364/OE.26.023397.
- [20] X. Ding *et al.*, "Improving the optical performance of multi-chip LEDs by using patterned phosphor configurations," *Optics Express*, vol. 26, no. 6, pp. 283–292, 2018, doi: 10.1364/OE.26.00A283.
- [21] A. D. Corbett *et al.*, "Microscope calibration using laser written fluorescence," *Optics Express*, vol. 26, no. 17, pp. 21887–21899, 2018, doi: 10.1364/OE.26.021887.
- [22] S. Kashima *et al.*, "Wide field-of-view crossed dragone optical system using anamorphic aspherical surfaces," *Applied Optics*, vol. 57, no. 15, pp. 4171–4179, 2018, doi: 10.1364/AO.57.004171.
- [23] G. Zhang, K. Ding, G. He, and P. Zhong, "Spectral optimization of color temperature tunable white LEDs with red LEDs instead of phosphor for an excellent IES color fidelity index," *OSA Continuum*, vol. 2, no. 4, pp. 1056–1064, 2019, doi: 10.1364/osac.2.001056.




- [24] Q. Xu, L. Meng, and X. Wang, "Nanocrystal-filled polymer for improving angular color uniformity of phosphor-converted white LEDs," *Applied Optics*, vol. 58, no. 27, pp. 7649–7654, 2019, doi: 10.1364/AO.58.007649.
- [25] Y.-C. Jen *et al.*, "Design of an energy-efficient marine signal light based on white LEDs," *OSA Continuum*, vol. 2, no. 8, pp. 2460–2469, 2019, doi: 10.1364/OSAC.2.002460.
- [26] Y. Sun, C. Zhang, Y. Yang, H. Ma, and Y. Sun, "Improving the color gamut of a liquid-crystal display by using a bandpass filter," *Current Optics and Photonics*, vol. 3, no. 6, pp. 590–596, 2019, doi: 10.3807/COPP.2019.3.6.590.

BIOGRAPHIES OF AUTHORS






Ha Thanh Tung    received the Ph.D degree in physics from University of Science, Vietnam National University Ho Chi Minh City, Vietnam, he is working as a lecturer at the Faculty of Basic Sciences, Vinh Long University of Technology Education, Vietnam. His research interests focus on developing the patterned substrate with micro and nano-scale to apply for physical and chemical devices such as solar cells, OLED, photoanode. He can be contacted at email: tunght@vlute.edu.vn.



Huu Phuc Dang    received a Physics Ph.D degree from the University of Science, Ho Chi Minh City, in 2018. Currently, he is a lecturer at the Faculty of Fundamental Science, Industrial University of Ho Chi Minh City, Ho Chi Minh City, Vietnam. His research interests include simulation LEDs material, renewable energy. He can be contacted at email: danghuuphuc@iuh.edu.vn.



Hoang Thinh Nhan    received his Engineer Diplom in Mechanical Engineering (Industrial Machines, Equipment and Process) from Ufa State Petroleum Technology University (USPTU), Russia, in 2003 and Ph.D Degree in Mechanical Engineering from USPTU in 2006. He is currently working as Vice Dean of Faculty of Engineering and Technology in the Nguyen Tat Thanh University, Ho Chi Minh City, Vietnam. His research interests include the renewable energy, optimisation techniques, hydraulic and pneumatic system, and offshore engineering. He can be contacted at email: htnhan@ntt.edu.vn.